

Ecological Responses of Autotrophic Microplankton to the Eutrophication of the Coastal Upwelling along the Southwest Coast of India

***¹Jyothibabu, R., ¹Karnan, C., ^{1,2}Jagadeesan, L., ¹Arunpandi, N., ¹Parthasarathi, S,**

¹Albin K Jose

¹CSIR-National Institute of Oceanography, Regional Centre, Kochi, India

²CSIR-National Institute of Oceanography, Regional Centre, Visakhapatnam, India

*Corresponding author. Telephone: +91 484 2390814; Fax: +91 484 2390618

*E-mail: rjyothibabu@nio.org

Abstract

The primary ecological effects of the eutrophication of upwelling in the nearshore waters are the triggering and sustenance of phytoplankton (diatom) blooms. Here, we present the changes in the morphological characteristics and body size of microautotrophs associated with the nutrient enrichment of coastal upwelling along the southwest coast of India. The FlowCAM data of microautotrophs representing two time-series locations in the coastal environment along the southwest coast of India at 18 weekly/biweekly frequencies showed the following features. The most significant response of the micro-autotrophs to the eutrophication associated with coastal upwelling during the Southwest Monsoon (June - September) was an increase in their mean bio-volume, either by increasing the individual cell size or by forming large colonies. During the Southwest Monsoon, large colonies of *Thalassiosira* (~8 cells/colony), *Thalassionema* (> 16 cells/colony), and *Asterionellopsis* (>8 cells/colony) become very abundant. *Streptotheca* formed large mat-like colonies (av. $192350 \pm 348 \mu\text{m}^3$ / individual), and *Fragilariopsis* grew as very long ribbons (av. $272997 \pm 5071 \mu\text{m}^3$ / individual). Large-sized *Chaetoceros* (av. $45715 \pm 1273 \mu\text{m}^3$ / individual) with longer setae were also plentiful during the Southwest Monsoon. All these changes in the morphology and life forms of microautotrophs would help them to rapidly assimilate nitrate under turbulent conditions during the Southwest Monsoon.

Keywords: Plankton, Phytoplankton, Upwelling, Southeastern Arabian Sea

1. Introduction

The Southeastern Arabian Sea (SEAS) is bounded on its east by the southwest coastline of India, which is known for its higher pelagic fishery resource availability compared to the rest of the Indian coast (Madhupratap et al., 2001). The coastal upwelling causes this unique fishery resource richness along the southwest coast of India during the Southwest Monsoon (Banse, 1959; Jyothibabu et al., 2008; Gupta et al., 2016; Karnan et al., 2017a). Although coastal upwelling regions account for only one percent of the ocean surface globally, they contribute roughly 50% of the world's fish landings (Mann, 1993). The upwelling causes nutrient enrichment in the surface waters and triggers high phytoplankton stock that is contributed mainly by diatoms; this favours the predominance of a short/traditional food chain, which is considered more efficient in transferring primary carbon to higher trophic levels (Mann, 1993). The SEAS is warmer ($>32^{\circ}\text{C}$) during the Pre-Southwest Monsoon (March-May) due to high solar insolation, which leads to thermally stratified and low nutrient surface layers supporting the growth of smaller diatoms, dinoflagellates, and phytoplankton (Asha Devi et al., 2010; Karnan et al., 2017a). By the commencement of coastal upwelling in June, the phytoplankton biomass (chlorophyll *a*) in the nearshore region enhances considerably, which continues in July through September. The high incidences of diatom blooms and high chlorophyll-*a* in the nearshore waters along the southwest coast of India during peak monsoon periods are indicative of the nutrient enrichment associated with upwelling (Madhupratap et al., 1990).

In 2014, we carried out several ecological studies at the time series locations of Alappuzha, along the southwest coast of India, as a part of the Alappuzha Mudbank Process Studies (AMPS). Some of the observations under this study elaborating upon various plankton ecological aspects are already published (Arunpandi et al., 2017; Karnan et al., 2017a; Karnan et al., 2017b; Jagadeesan et al., 2017; Jyothibabu et al., 2018a; Jyothibabu et al., 2018b; Jyothibabu et al., 2018c). During this study, a FlowCAM was extensively used to quantify various plankton components and to explain how the plankton community responded to the hydrological changes on a spatiotemporal scale. They found coastal upwelling during the Southwest Monsoon to be the most crucial factor impacting the plankton components in the study region. Similarly, the mean size of the micro-autotrophs increased noticeably during the Southwest Monsoon (Karnan et al., 2017a). There was a marked increase in the abundance of large-sized, chain-forming diatoms. However, whether this change was a compositional shift or an increase in the size of individual phytoplankton could not be ascertained. It is mainly required to understand how phytoplankton, the fabric of an essential food chain, responds to nutrient enrichment during upwelling. Hence, the objective of this paper is to explain how micro-

plankton adapts to size variations under nutrient-enriched conditions that attract massive shoals of small pelagic fisheries along the southwest coast of India during the Southwest Monsoon. To explain this, we used the FlowCAM data of microplankton from the study region and analysed the mode of increase of microplankton size with time. We also attempted to track the changes in microplankton cell size and growth form as the ecological indicators of upwelling.

2. Materials and Methods

The study area in the coastal waters of Alappuzha is in the Southeastern Arabian Sea. The samples for physicochemical and biological parameters were collected from two locations outside (M1) and inside (M2), the Alappuzha mud banks, along the southwest coast of India. This study encompasses a total of 18 weekly/biweekly sampling from the Pre-Monsoon (April) to the late Southwest Monsoon (September) of 2014 (Figure 1). Both sampling locations (M1 and M2) were at a depth of 7 m and separated by around 8 km. The physical properties of the water column (temperature and salinity) and chlorophyll-*a* concentration were measured using a CTD profiler (Seabird electronics, USA), and water samples were collected using Niskin bottles to quantify the macronutrients, chlorophyll-*a* using a laboratory fluorometer and microplankton. Nutrients were measured using the standard procedure (Grasshoff, 1983), and chlorophyll *a* was measured using a laboratory fluorometer (Trilogy, Turner designs, USA) following JGOFS methods (UNESCO, 1994).

Water samples for microplankton (200-1000 ml) were gently filtered through a 300 µm nylon mesh to remove the larger particles and analysed through a portable FlowCAM (Fluid Imaging Technologies, USA) following standard procedure (Karnan et al., 2017a). FlowCAM enables to quantify live microplankton and also capture their colour and morphological features (Zarauz and Irigoien, 2008). With the help of FlowCAM, we could analyse the live plankton within a few hours of sample collection from the study sites (Zarauz and Irigoien, 2008; Karnan et al., 2017a). The FlowCAM magnification was set at 40X in laser trigger mode (525 nm) to capture the images of live plankton (Sieracki et al., 1998; Zarauz and Irigoien, 2008; Alvarez et al., 2012; Karnan et al., 2017a), and identified using relevant literature (Tomas, 1996). The FlowCAM-analysed samples were collected in separate vials and observed under an inverted microscope for the confirmation of microplankton species. Monitoring of the composition, body size, and changes in morphological features of microplankton communities during the Southwest Monsoon in comparison with the Pre-monsoon produced some interesting observations from this region. Multiple correlation analyses using Exel Stat Pro was carried out to understand the correlations between relevant biological and environmental variables.

3. Results and Discussion

Significant enhancement in phytoplankton blooms is quite usual in the southwest coast of India during the Southwest Monsoon associated with the coastal upwelling, which also causes a drop in seasonal SST (Figure 2). The weekly time series data presented in this paper provide a general description of the changes in the physicochemical parameters and nutrient ratios of respective seasons (Table 1). The warm and oligotrophic waters of the present study region during the Pre-Monsoon season gets replaced by the cold and more nutrient-rich upwelled waters with the onset of the Southwest Monsoon (Karnan et al., 2017a; Jagadeesan et al., 2017). The silicate concentration was always high (7.9-14.4 μM) in the study region, due to its proximity to the coast. There was a significant increase in the abundance, size, and biomass of autotrophic plankton communities during the upwelling/Southwest Monsoon period when the nitrate concentration increased (Table 1). The nutrient ratios of $\text{N/Si} < 0.5$ and $\text{N/P} < 5$ (Table 1) are indicative of a significant nitrogen deficiency in the sampling domain during Pre-Monsoon (Redfield et al., 1963; Harrison et al., 1977; Paul et al., 2008). However, these ratios increased during the Southwest Monsoon due to the introduction of nitrate through coastal upwelling (Table 1). A corresponding decrease in silicate during the Southwest Monsoon could be indicative of its better assimilation by phytoplankton, especially large-sized diatoms during upwelling.

During the Southwest Monsoon of the present study, as expected, coastal upwelling occurred in both M1 and M2 (Figure 3), which implied a possible onshore advection of the subsurface waters, including microplankton (Peterson, 1998). The resultant nitrate enrichment in the nearshore waters noticeably increased the phytoplankton biomass (chlorophyll *a*) enormously in both the locations (Figure 4). The growth of large diatoms causes a significant enhancement of chlorophyll-*a* in the sampling domain during the Southwest Monsoon (Figure 4; Jyothibabu et al., 2018a; Jyothibabu et al., 2018b). The lowering of the Si/P ratio during the Southwest Monsoon is due to the efficient utilization of silicate by diatoms during bloom formation. Though the upwelling process is discernible in early June in the nearshore waters, its intensity was maximum during late June, as evident from the maximum cooling (25°C) of subsurface waters in the region (Karnan et al., 2017a). Thus, the increase in chlorophyll-*a* in the study region coincided with the period of maximum cooling in July (Table 1). The interrelationship between the biological and environmental variables is very clear in the RDA triplot (Figure 5).

To explain how the phytoplankton body size increased in the study area during the Southwest Monsoon, FlowCAM, and microscopy data were carefully analysed. Altogether, 88 species of microautotrophs inhabited in the study area during the present sampling (Supplementary Table 1). It

was apparent that there was no significant shift in the composition of microplankton in the study area between the Pre-Monsoon and the Southwest Monsoon period. On the other hand, there was a considerable increase in the abundance and size of microplankton, such as *Fragilariopsis* sp., *Coscinodiscus* sp., *Asterionellopsis* sp., *Rhizosolenia* sp., and *Thalassionema* sp. during the Southwest Monsoon (Table 2). This increase was partly due to the changes in the morphological features of phytoplankton in response to nitrate enrichment (Table 3). The FlowCAM images (Figure 6) illustrate the salient differences in the dominant plankton communities during the Southwest Monsoon. Marine diatoms exhibit large morphological variability from solitary to chain or colony-forming species, with each cell shape ranging from spherical to cylindrical and elongate pennate (Takabayashi et al., 2006). Each shape and size of diatoms has apparent advantages and disadvantages in terms of suspension in the water column, nutrient uptake, light absorption, and predator avoidance (Smayda, 1970; Fogg, 1991; Smayda and Boleyn, 1996; Takabayashi et al., 2006).

The changes in size, morphology, and living habit (solitary or colonial) of phytoplankton, especially of diatoms, during the Southwest Monsoon, was very significant (Figure 7a – j). The diatom *Thalassiosira* sp., present as individual cells during Pre-Southwest Monsoon (Figure 7a), and formed colonies of > 4 cells during the Southwest Monsoon (Figure 5f). Similarly, another diatom *Fragilaria* sp., present in meager numbers and very small chains during the Pre-Monsoon (Figure 5b), was found to transform into rather long and expansive chains during Southwest Monsoon (Figure 5g). The cells of *Thalassionema nitzschioides*, present in small colonies of < 4 cells during the Pre-Southwest Monsoon (Figure 5c), were transformed into extended chains of > 16 cells during Southwest Monsoon (Figure 5h). The single-celled *Streptotheca* sp. of the Pre-Monsoon period transformed into longer bands during the Southwest Monsoon (Figure 5i). Similarly, the short-chained *Asterionellopsis* sp. of the Pre-Monsoon period changed to long spirals of > 30 cell chains during the Southwest Monsoon (Figure 5j). *Chaetoceros* sp., and *Bacteriastrum* sp., present in a small cellular form with short setae during the Pre-monsoon, enlarged their size and setae length during the Southwest Monsoon (Figure 6a). Though the smaller dinoflagellates *Ceratium furca* and *C. fusus* were dominant throughout the study, an increase in the abundance of large-sized species *C. macroceros* and *C. tropos*, in the form of long chains, was observed during the Southwest Monsoon (Figure 6d). In essence, in a situation of a rapid increase in nitrate concentration, the microautotrophs were effective in assimilating them by increasing their cell size as well as by forming long chains of colonies, mats, and ribbons, thereby increasing the mean size of microplankton in the study area (Table 3).

The changes in the size, morphology, and living habit (solitary or colonial) of the microplankton, as observed above, could be the adaptation of plankton under specialized environmental situations such as in the zones of upwelling and gyres (Estrada and Berdalet, 1997). The southwest coast of India has heavy winds ($> 6 \text{ ms}^{-1}$) and rough Sea during the Southwest Monsoon (Muraleedharan et al., 2017; Samiksha et al., 2017). The high turbulence is a disturbance to the smaller and single-celled plankton community that cannot assimilate nutrients for their growth (Barton et al., 2014). The phytoplankton overcomes such turbulent conditions by increasing their cell volume and by forming colonies, chains, mats, and ribbons to effectively get stabilized and utilize nutrients (Karp-Boss et al., 1996). The large-sized phytoplankton also exhibits increased nutrient assimilating capacity under turbulent conditions (Karp-Boss et al., 1996; Peters et al., 2006; Barton et al., 2014). At a particular level of turbulence, oscillating flow along different parts of a microplankton chain increases nutrient uptake as a function of the chain length (Pahlow et al., 2017). Modifications of the morphological features such as longer horns and longer spines could also facilitate an increased surface area of micro-autotrophs for better nutrient uptake and flotation (Smayda and Boleyn, 1965; Fryxell et al., 1984).

Large surface area could also enable the micro-autotrophs to harvest maximum solar radiation, which is relatively low in the study area during the Southwest Monsoon (Karnan et al., 2017a; Jyothibabu et al., 2018a). Alternatively, a decrease in silicate during the Southwest Monsoon of the present study could also indicate the possibility that longer chains favoured during turbulence upon silica depletion (Dell'Aquila et al., 2017). Since the current study area is in the tropics, an increase in temperature (from 6 to 17°C) favouring long chains of diatom, as observed by Takabayashi et al. (2006), might not be exactly applicable in the present case. At the same time, it is not clear in this study whether a temperature drop of 5-7 °C in the water column during the coastal upwelling during the Southwest Monsoon has an inducing effect on the morphological modifications of micro-autotrophs discussed here. To conclude, we propose that the change in the morphology, increase in isolated cell size and increase in the size of the colonies of micro-autotrophs, as observed in this study, can be considered as the best ecological responses of upwelling by phytoplankton in the nearshore waters along the Southwest coast of India.

Phytoplankton size increases along the southwest coast of India during the Southwest Monsoon, which is generally believed a consequence of the phytoplankton compositional shift (Banse et al., 1984). But this study in the nearshore waters along the southwest coast of India showed that the microautotroph compositional change between the Pre-Monsoon and the Southwest Monsoon is not so significant. In contrast, the increase in the size of the individual species and colonial living habits

(solitary to colonial and single or a few cells large elongated chains of cells) of many microautotrophs, such as *Fragilariopsis* sp., *Coscinodiscus* sp., *Asterionellopsis* sp., *Rhizosolenia* sp., and *Thalassionema* sp. causes a significant increase in the overall size of the phytoplankton during the Southwest Monsoon (Table 2). The implication of the enhancement in the body size of the phytoplankton in the food chain and regional fisheries could be summarised logically (Figure 8). Large or chain-forming phytoplankton abundant during the Southwest Monsoon facilitates the shortest food chain, phytoplankton to fish, which increases the transfer efficiency, thereby supporting considerable fishery resources (Mann et al., 1993). On the other hand, smaller, single-celled phytoplankton during the Pre-Southwest Monsoon, is mostly transferred to fishes primarily through zooplankton, which is one step longer than the direct transfer of phytoplankton carbon biomass to fishes. Therefore, one of the reasons behind high fishery stock availability along the southwest coast of India during the Southwest Monsoon period may be through the increased size attained from morphological modifications and living habits of microplankton favouring the shortest possible food chain in the region.

4. Conclusion

This study presented advanced FlowCAM-based measurements of the autotrophic microplankton community in two selected time-series locations along the southwest coast of India to explain how they respond to the eutrophication associated with coastal upwelling. The size of autotrophic microplankton increased during the Southwest Monsoon (upwelling) period through (a) enlargement of individual plankton cells and (b) formation of long-chain colonies of microplankton. FlowCAM data revealed that during the Southwest Monsoon, *Thalassiosira* sp., formed colonies of around eight cells, *Streptothecca* sp. formed long mat-like structures, *Fragilariopsis* occurred as longer ribbons. *Thalassionema nitzschioides* and *Asterionellopsis* sp. formed extended colonies > 16 and > 30 cells, respectively. *Chaetoceros* sp. and *Bacteriastrum* sp. grew in size with longer setae during the nutrient enrichment associated with coastal upwelling. This increase in size and length was due to the adaptation of the microplankton community to turbulent conditions for better assimilation of nutrients, which are their clear ecological responses to nutrient enrichment due to coastal upwelling. And these responses of microplankton in the nearshore waters facilitate the shortest foodchain facilitating the most efficient transfer of organic carbon to fishes favouring large fish stock available in the vicinity, which may be true to similar coastal zones across the globe.

Acknowledgments

The authors thank the former and the present Directors of CSIR - National Institute of Oceanography (NIO), India, for the facilities. We are thankful to all colleagues in CSIR-NIO and ICAR-CMFRI

India, who were a part of the Alappuzha Mudbank Process Studies. Karnan thanks CSIR - India for the CSIR- JRF research fellowship during the study period. This is CSIR-NIO contribution.....

References

- Alvarez, E., Lopez-Urrutia, A., Nogueira, E., 2012. Improvement of plankton biovolume estimates derived from image-based automatic sampling devices: application to FlowCAM. *Journal of plankton research* 34, 454-469.
- Arunpandi, N., Jyothibabu, R., Jagadeesan, L., Gireeshkumar, T.R., Karnan, C., Naqvi, S.A., 2017. Noctiluca and copepods grazing on the phytoplankton community in a nutrient-enriched coastal environment along the southwest coast of India. *Environmental Monitoring and Assessment* 189, 351.
- Asha Devi, C.R., Jyothibabu, R., Sabu, P., Jacob, J., Habeebrehman, H., Prabhakaran, M.P., Jayalakshmi, K.J., Achuthankutty, C.T., 2010. Seasonal variations and trophic ecology of microzooplankton in the southeastern Arabian Sea. *Continental Shelf Research* 30, 1070–1084.
- Banse, K., 1959. On upwelling and bottom-trawling off the southwest coast of India. *Journal of the Marine Biological Association of India* 1, 33-49.
- Barton, A.D., Ward, B.A., Williams, R.G., Follows, M.J., 2014. The impact of fine-scale turbulence on phytoplankton community structure. *Limnology and Oceanography: Fluids and Environments* 4, 34-49.
- Dell'Aquila, G., Ferrante, M. I., Gherardi, M., Lagomarsino, M. C., Ribera d'Alcalà, M., Iudicone, D., Amato, A., 2017. Nutrient consumption and chain tuning in diatoms exposed to storm-like turbulence. *Scientific Reports* | 7: 1828 | DOI:10.1038/s41598-017-02084-6.
- Estrada, M., Berdalet, E., 1997. Phytoplankton in a turbulent world. *Scientia Marina* 61, 125-140.
- Fogg, G.E., 1991. The phytoplanktonic way of Life. *New Phytology* 118 (2), 191-232.
- Fryxell, G.A., Gould Jr, R.W., Watkins, T.P., 1984. Gelatinous colonies of the diatom *Thalassiosira* in Gulf Stream Warm Core Rings including *T. fragilis*, sp. nov. *British Phycological Journal* 19, 141-156.
- Grasshoff, K., 1983. Methods of Seawater Analysis. In K. Grasshoff, Ehrhardt, M., Kremling, K., (Ed.) Weinheim, Verlag Chemie, pp. 419.
- Gupta, G.V.M., Sudheesh, V., Sudharma, K.V., Saravanane, N., Dhanya, V., Dhanya, K.R., Lakshmi, G., Sudhakar, M., Naqvi, S.W.A., 2016. Evolution to decay of upwelling and associated biogeochemistry over the southeastern Arabian Sea shelf. *Journal of Geophysical Research: Biogeosciences* 121, 159-175.
- Harrison, P.J., Conway, H.L., Holmes, R.W., Davis, C.O., 1977. Marine diatoms grown in chemostats under silicate or ammonium limitation. III. Cellular chemical composition and morphology of *Chaetoceros debilis*, *Skeletonema costatum*, and *Thalassiosira gravida*. *Marine Biology* 43, 19-31.
- Jagadeesan, L., Jyothibabu, R., Arunpandi, N., Karnan, C., Balachandran, K.K., 2017. Dominance of coastal upwelling over Mud Bank in shaping the mesozooplankton along the southwest coast of India during the Southwest Monsoon. *Progress in Oceanography* 156, 252-275.

- Jyothibabu, R., Arunpandi, N., Karnan, C., Jagadeesan, L., Manojkumar, T.M., Balachandran, K.K., Naqvi, S.W.A., 2018b. *Fragilariopsis* sp. bloom causes yellowish-brown waters off Alappuzha, south-central Kerala coast, India, during the mud bank-upwelling phase. *Current Science* 115, 152-159.
- Jyothibabu, R., Balachandran, K.K., Jagadeesan, L., Karnan, C., Arunpandi, N., Naqvi, S.W.A., Pandiarajan, R.S., 2018a. Mud Banks along the southwest coast of India are not too muddy for plankton. *Scientific Reports* 8, 2544.
- Jyothibabu, R., Devi, C.R.A., Madhu, N.V., Sabu, P., Jayalakshmy, K.V., Jacob, J., Habeebrehman, H., Prabhakaran, M.P., Balasubramanian, T., Nair, K.K.C., 2008. The response of microzooplankton (20-200 μ m) to coastal upwelling and summer stratification in the southeastern Arabian Sea. *Continental Shelf Research* 28, 653-671.
- Jyothibabu, R., Jagadeesan, L., Karnan, C., Arunpandi, N., Pandiarajan, R.S., Balachandran, K.K., 2018c. Ecological Indications of Copepods to Oxygen-deficient Near-shore Waters, *Ecological Indicators* 93, 76-90.
- Karnan, C., Jyothibabu, R., Arunpandi, N., Jagadeesan, L., Muraleedharan, K.R., Pratihari, A.K., Balachandran, K.K., Naqvi, S.W.A., 2017a. Discriminating the biophysical impacts of coastal upwelling and mud banks along the southwest coast of India. *Journal of Marine Systems* 172, 24-42.
- Karnan, C., Jyothibabu, R., Kumar, T.M.M., Balachandran, K.K., Arunpandi, N., Jagadeesan, L., 2017b. Seasonality in Autotrophic Mesoplankton in a Coastal Upwelling-mud bank Environment along the Southwest Coast of India and its Ecological Implications. *Continental Shelf Research* 146, 1-12.
- Karp-Boss, L., Boss, E., Jumars, P.A., 1996. Nutrient fluxes to planktonic osmotrophs in the presence of fluid motion. *Oceanography and Marine Biology: an Annual Review* 34, 71-107.
- Madhupratap, M., Nair, K.N.V., Gopalakrishnan, T.C., Haridas, P., Nair, K.K.C., Venugopal, P., Gauns, M., 2001. Arabian Sea oceanography and fisheries of the west coast of India. *Current Science* 81, 355-361.
- Madhupratap, M., Nair, S.R.S., Haridas, P., Padmavati, G., 1990. Response of zooplankton to physical changes in the environment: coastal upwelling along the central west coast of India. *Journal of Coastal Research* 413-426.
- Mann, K. H., 1993. Physical oceanography, food chains, and fish stocks: a review. *ICES Journal of Marine Sciences*, 50, 105 - 119.
- Muraleedharan, K.R., Kumar, P.K.D., Kumar, S.P., Srijith, B., John, S., Kumar, K.R.N., 2017. Observed salinity changes in the Alappuzha mud bank, southwest coast of India and its implication to hypothesis of mudbank formation. *Continental Shelf Research* 137, 39-45.
- Pahlow, M., Riebesell, U., Wolf-Gladrow, D. A. 2017. Impact of cell shape and chain formation on nutrient acquisition by marine diatoms. *Limnology and Oceanography* 42, 1660-1672, doi:10.4319/lo.1997.42.8.1660 (1997).
- Paul, J.T., Ramaiah, N., Sardesai, S., 2008. Nutrient regimes and their effect on distribution of phytoplankton in the Bay of Bengal. *Marine Environmental Research* 66, 337-344.
- Peters, F., Arin, L., Marrase, C., Berdalet, E., Sala, M.M., 2006. Effects of small-scale turbulence on the growth of two diatoms of different size in a phosphorus-limited medium. *Journal of Marine Systems* 61, 134-148.
- Peterson, W., 1998. Life cycle strategies of copepods in coastal upwelling zones. *Journal of Marine Systems*, 15, 313-326.

- Redfield, A.C., Ketchum, B.H., Richards, A., 1963. The influence of organisms on the composition of sea water. In: Hill, M.M. (Ed.), *The Sea*, vol. 2. Interscience, pp. 26-77.
- Samiksha, S.V., Vethamony, P., Rogers, W.E., Pednekar, P.S., Babu, M.T., Kumar, P.K.D., 2017. Wave energy dissipation due to mudbanks formed off southwest coast of India. *Estuarine, Coastal and Shelf Science* 196, 387-398.
- Sieracki, C.K., Sieracki, M.E., Yentsch, C.S., 1998. An imaging-in-flow system for automated analysis of marine microplankton. *Marine Ecology Progress Series* 168, 285-296.
- Smayda, T.J., Boleyn, B.J., 1965. Experimental observations on the flotation of marine diatoms. I. *Thalassiosira* CF *nana*, *Thalassiosira rotula* and *Nitzschia seriata*. *Limnology and Oceanography* 10, 499-509.
- Smayda, T.J., Boleyn, B.J., 1966. Experimental observations on the floatation of marine diatoms II. *Skeletonema costatum* and *Rhizosolenia setigera*. *Limnology and Oceanography* (1), 18-34.
- Smyda, T.J., 1970. The suspension and sinking of phytoplankton in the Sea. *Oceanography and Marine Biology Annual Review* 8, 353-414.
- Takabayashi, M., Lew, K., Johnson, A., Marchi, A. L., Dugdale, R., & Wilkerson, F. P., 2006. The effect of nutrient availability and temperature on chain length of the diatom, *Skeletonema costatum*. *Journal of Plankton Research*, 28, 831-840.
- Tomas, C.R., 1996. *Identifying marine diatoms and dinoflagellates*, edited by: Tomas, C.R. Academic Press, Inc., San Diego, California.
- UNESCO, 1994. *Protocols for the Joint Global Ocean Flux Study, Manual and Guides*, vol. 29, p. 170.
- Zarauz, L., Irigoien, X., 2008. Effects of Lugols fixation on the size structure of natural nano microplankton samples, analyzed by means of an automatic counting method. *Journal of plankton research* 30, 1297-1303.

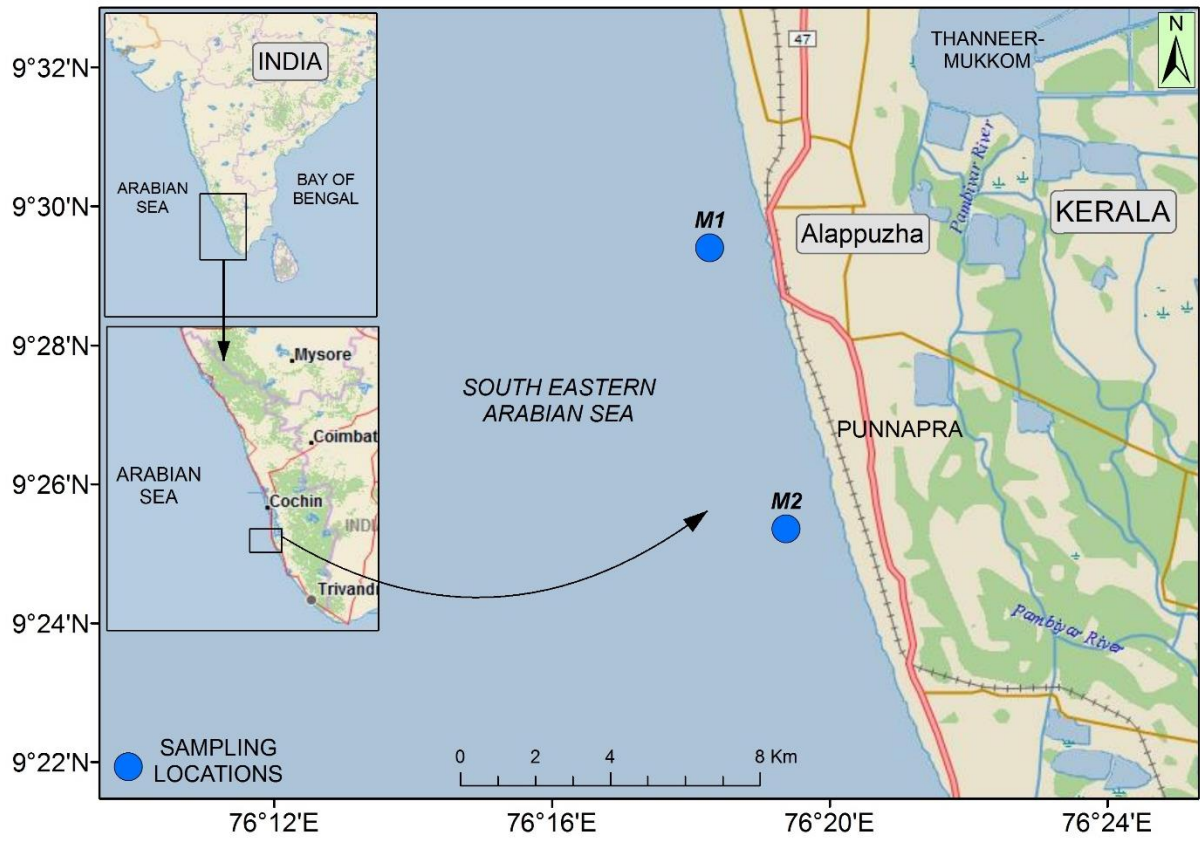


Figure 1 - Sampling area situated along the Southwest (Kerala) coast of India. The blue circles are the sampling locations from where 18-time series weekly/biweekly samples were collected.

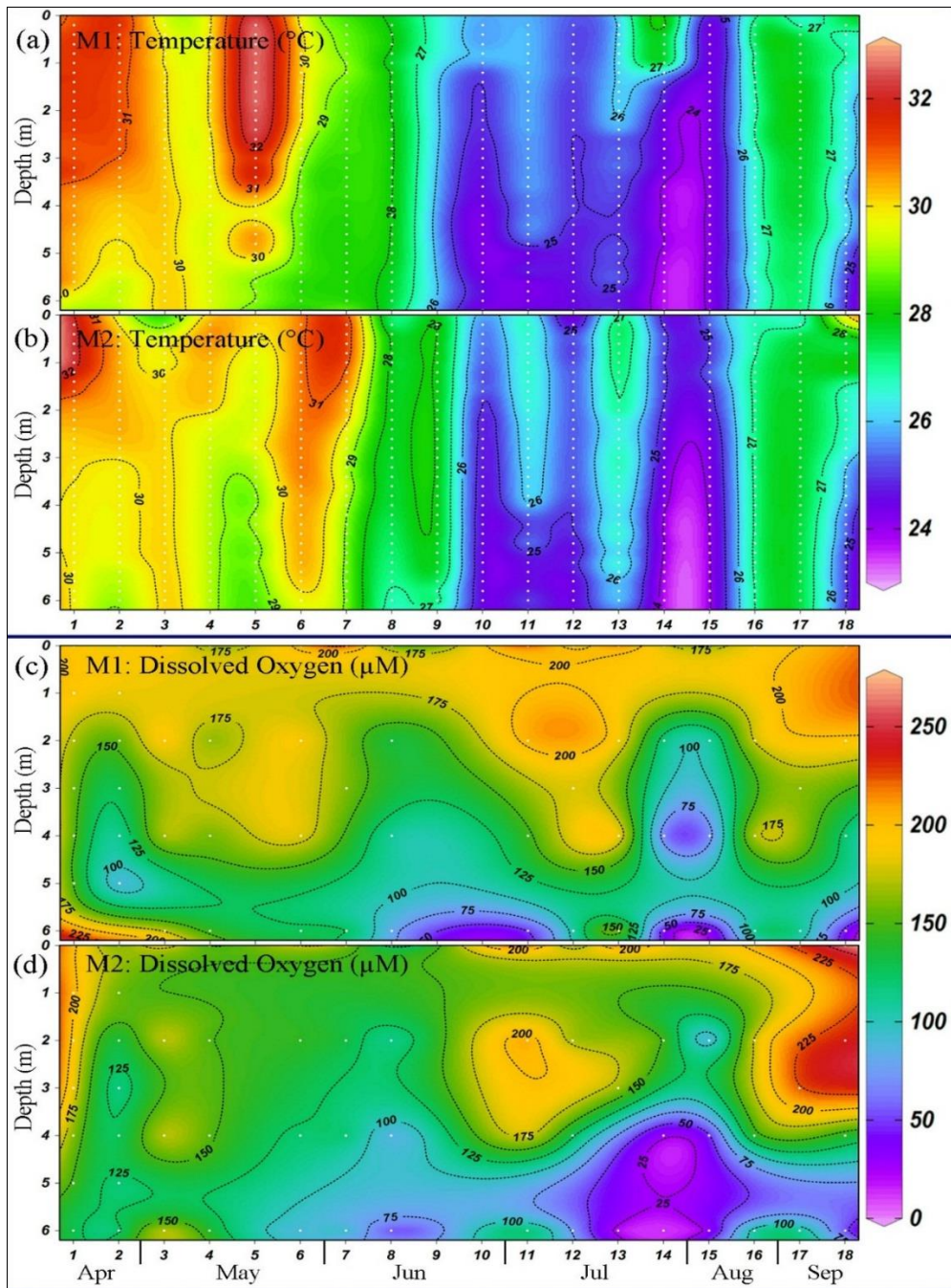


Figure 2 - Vertical distribution of (a&b) temperature and (c &d) dissolved oxygen in M1 and M2 locations. Signatures of coastal upwelling such as surfacing of cold and oxygen-deficient waters are evident in both sampling locations during the Southwest Monsoon (June - September).

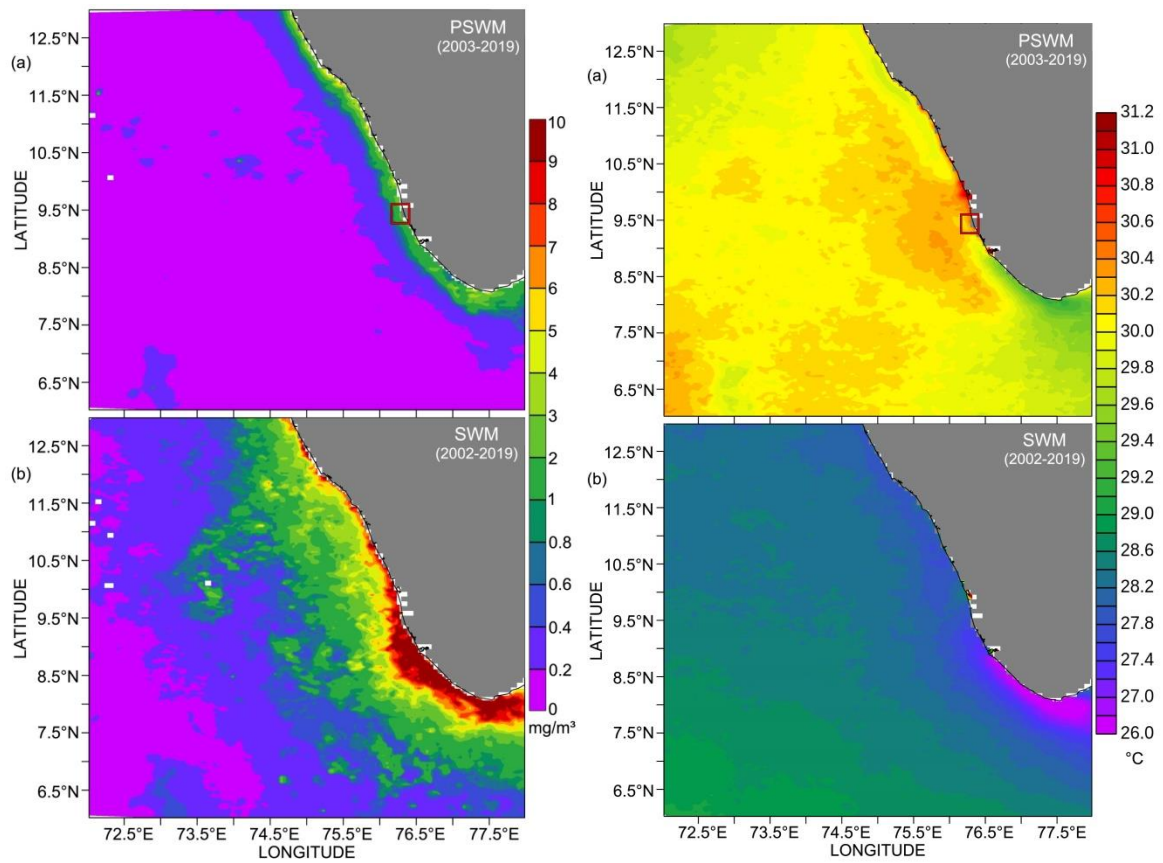


Figure 3 - (a & b) Enhancement of phytoplankton biomass (chlorophyll-*a*) and (c) and (d) decrease in Sea surface temperature in the South-eastern Arabian Sea during the Southwest Monsoon associated with the coastal upwelling.

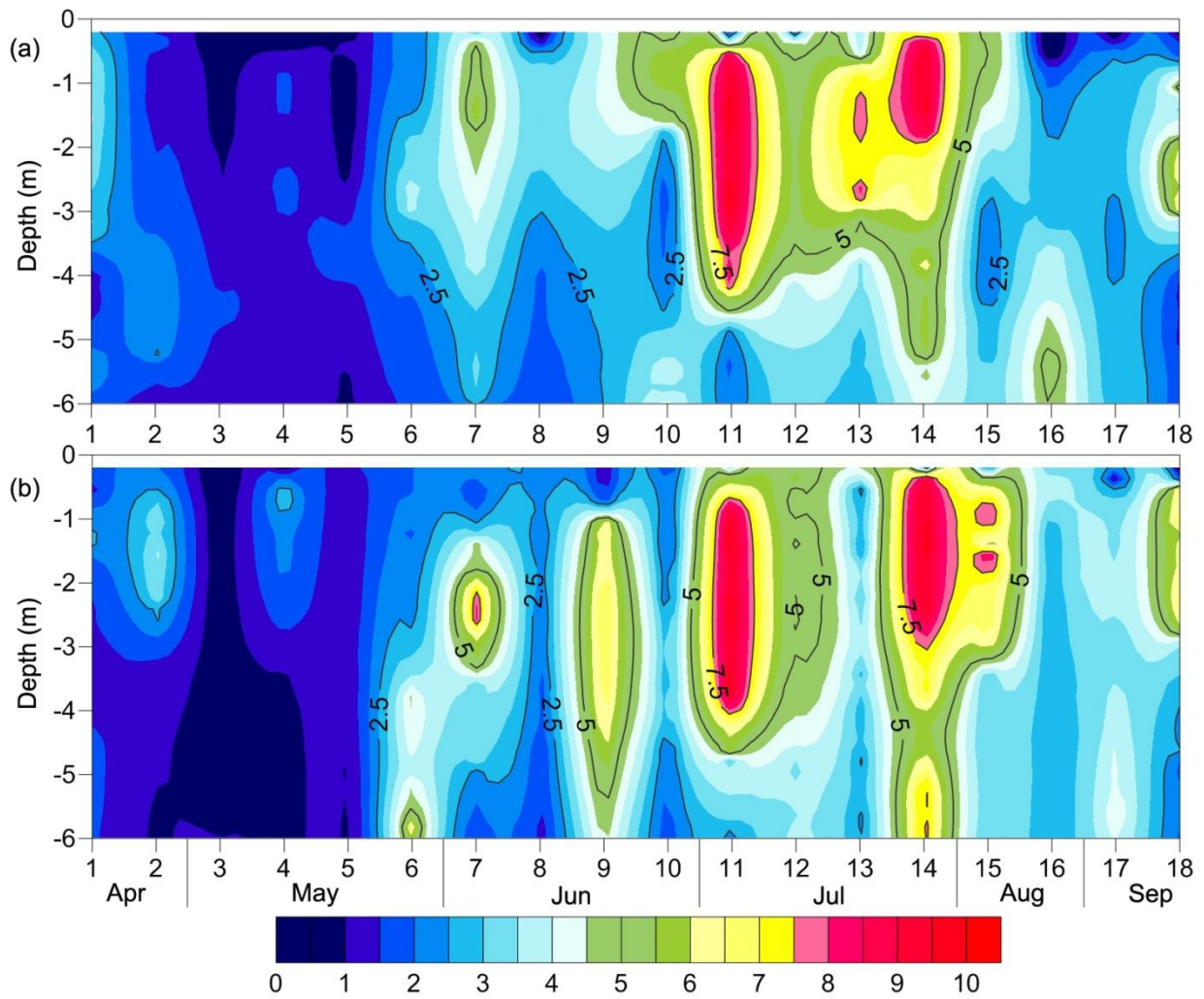


Figure 4 - The vertical distribution of chlorophyll-*a* (mg/ m³) concentration in M1 and M2 locations in the nearshore waters along the southwest coast of India. In this figure, CTD chlorophyll *a* data was corrected with the laboratory flourometer following the procedure of Jyothibabu et al., 2012.

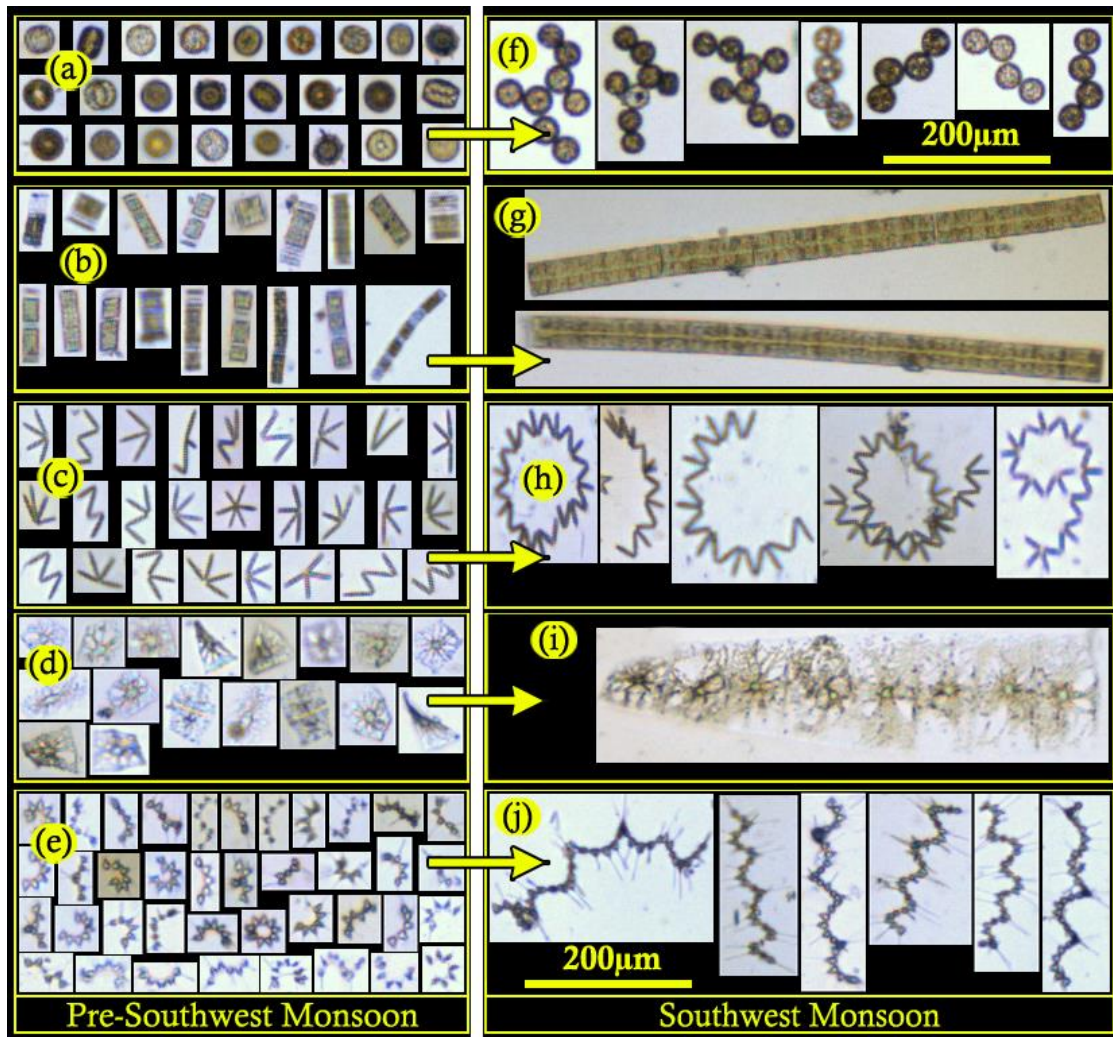


Figure 5 - Morphological modifications of microautotrophs associated with nutrient enrichment in the nearshore waters along the southwest coast of India during the Southwest Monsoon. The left side panel of FlowCAM images showing the (a) individual cells of *Thalassiosira* sp., (b) smaller chains of *Fragilariopsis oceanica*, (c) smaller colonies of *Thalassionema nitzschioides* (d) individual cells of *Streptotheca* sp., (e) smaller colonies of *Asterionellopsis* sp., found during Pre-Southwest Monsoon and the right-side panel (f-j) presenting the structural modifications (extensive colonies, longer chains, and filaments) and dominance of larger sized species of the respective plankton genera during the Southwest Monsoon.

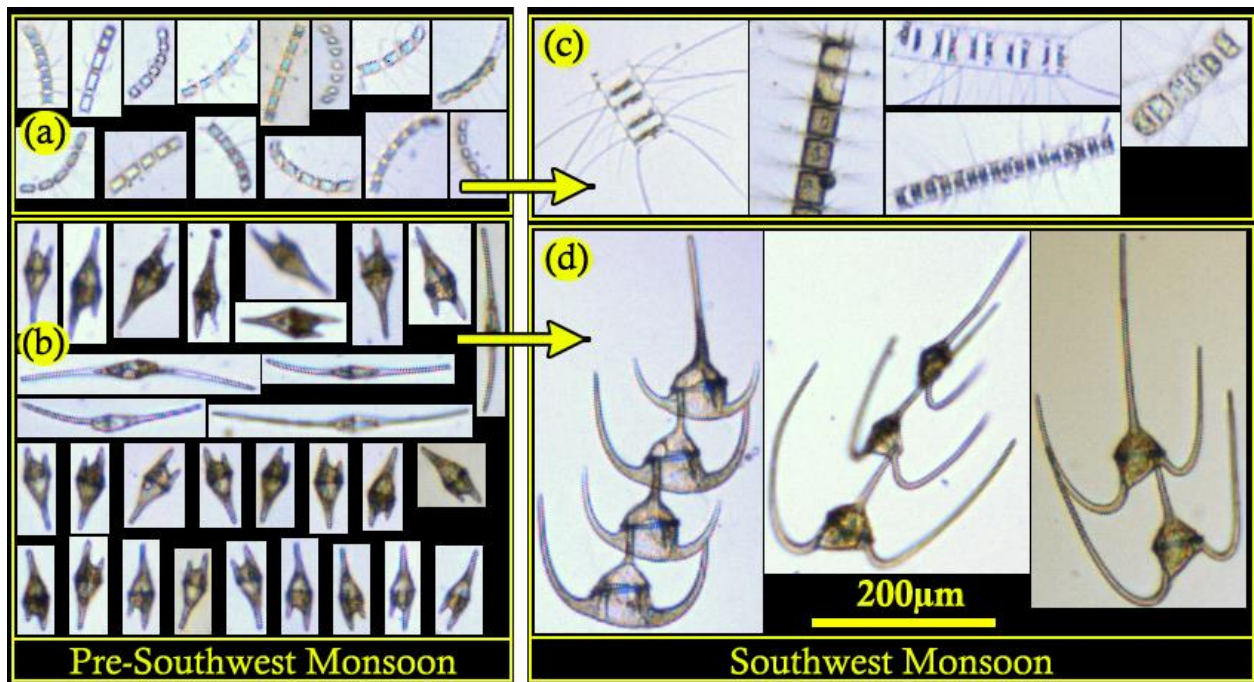


Figure 6 - Microautotrophs compositional change as a response to nutrient enrichment in the nearshore waters associated with the coastal upwelling during the Southwest Monsoon. The left side panel of FlowCAM images showing (a) *Chaetoceros* species with relatively smaller cells and shorter setae, and (b) smaller sized *Ceratium* species (*C. furca* and *C. fusus*) found during Pre-Southwest Monsoon. The right-side panel (c-d) shows *Chaetoceros* species with longer filaments, setae, and larger species of *Ceratium* forming longer chains during the Southwest Monsoon.

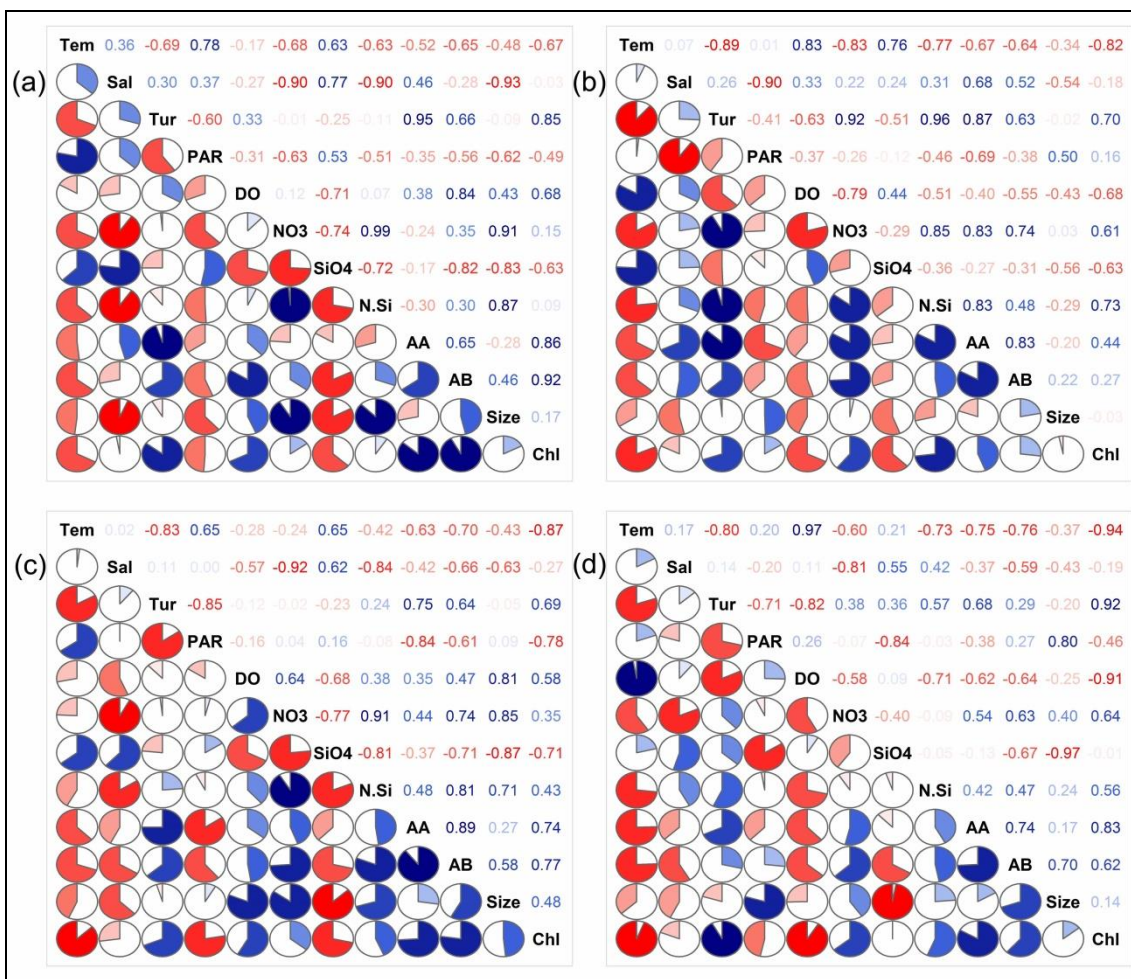


Figure 7 - Graph of multiple correlations between environmental and biological parameters during (a) & (b) surface and subsurface waters in M1 and (c) and (d) surface and subsurface waters in M2 locations. Increasing colour gradients in circles and numbers are the increasing significance of correlation.

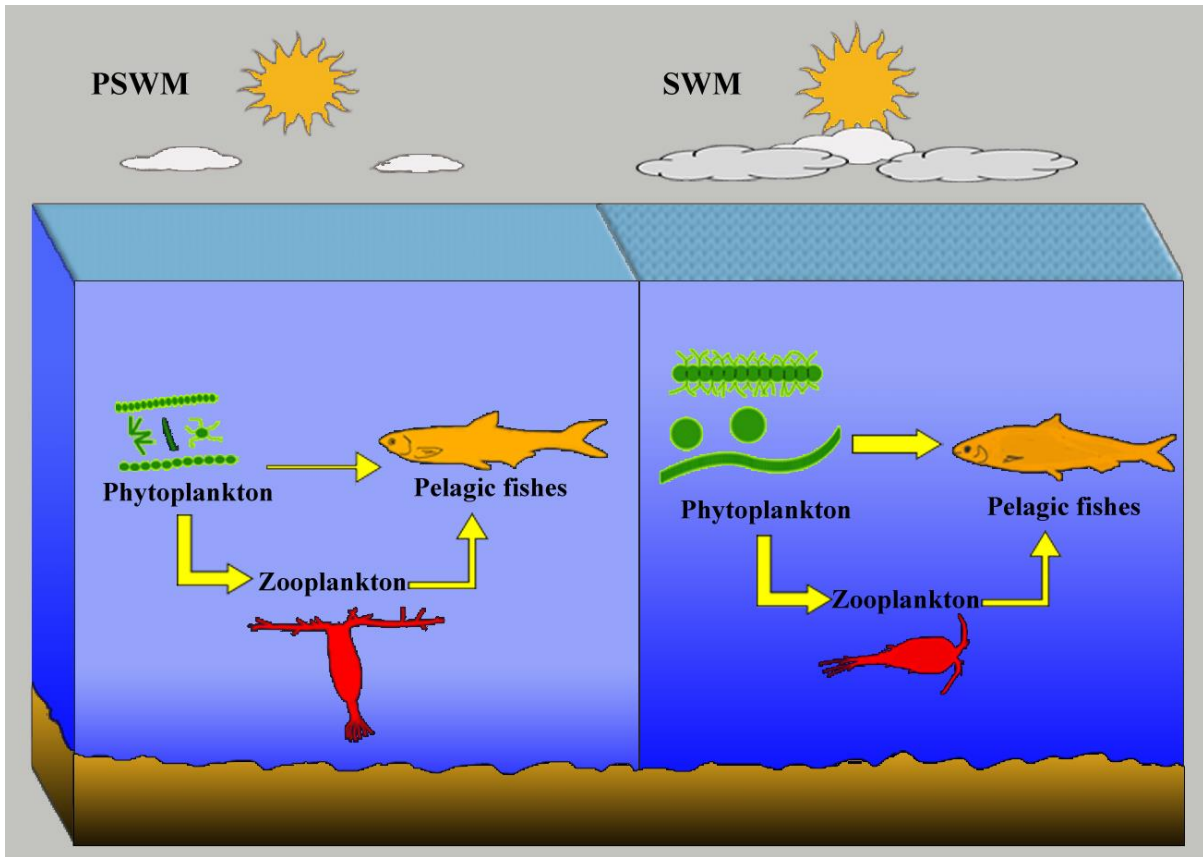


Figure 8 - Schematic of the dominant modes of nutrition to fishes in the present study area during the Pre-Southwest Monsoon (PSWM) and Southwest Monsoon (SWM). Though traditional food web was dominant during both seasons, the shortest food chain was dominant during the SWM effecting more efficient transfer of primary organic carbon to the fishes in the higher trophic level.

Table 1 - Seasonal variation of physicochemical parameters in the surface and sub-surface waters of sampling locations. The values presented as mean \pm SE. Abbreviations: PSWM - Pre-Southwest Monsoon, SWM - Southwest Monsoon

Surface (1m)	Location M1		Location M2	
Parameters	PSWM	SWM	PSWM	SWM
Temperature	31 \pm 0.3	26.7 \pm 0.4	30.7 \pm 0.6	27 \pm 0.6
Salinity	34.3 \pm 0.1	33.6 \pm 0.5	34.3 \pm 0.2	34 \pm 0.3
NO ₃ (μ M/L)	0.7 \pm 0.5	2 \pm 0.7	0.7 \pm 0.5	3.1 \pm 1.3
PO ₄ (μ M/L)	0.6 \pm 0.1	0.9 \pm 0.2	0.6 \pm 0.1	0.9 \pm 0.1
SiO ₄ (μ M/L)	13.3 \pm 2.9	7.9 \pm 1.7	13.8 \pm 3.9	8.8 \pm 2
N:Si	0.1	0.3	0.1	0.4
N:P	1.2	2.2	1.2	3.4
Si:P	22	8.8	23	9.8
Chl-a (μ g/L)	2.4 \pm 0.9	5.8 \pm 2.1	2.7 \pm 1.02	6.02 \pm 1.4
Subsurface (5m)	Location M1		Location M2	
Parameters	PSWM	SWM	PSWM	SMW
Temperature	29.9 \pm 0.3	25.8 \pm 1.04	29.7 \pm 0.16	26 \pm 1
Salinity	34.5 \pm 0.02	34.5 \pm 0.37	34.6 \pm 0.13	34.3 \pm 0.6
NO ₃ (μ M/L)	2.1 \pm 0.6	4.2 \pm 0.9	1.9 \pm 0.4	5 \pm 1
PO ₄ (μ M/L)	0.9 \pm 0.1	1.1 \pm 0.2	0.7 \pm 0.1	1.2 \pm 0.1
SiO ₄ (μ M/L)	14.4 \pm 3.1	10.2 \pm 1.8	12.3 \pm 2.4	12.7 \pm 1.7
N:Si	0.1	0.4	0.2	0.4
N:P	2.3	3.8	2.7	4.2
Si:P	16	9.3	18	11
Chl-a (μ g/L)	2.23 \pm 0.6	3.54 \pm 0.9	1.87 \pm 0.16	3.8 \pm 0.73

Table 2 – Micro-autotrophs recorded during the study. \$\$, **, and ## represent the species found only during the Premonsoon, the Southwest Monsoon, and both seasons, respectively.

Sl. No.	Micro-autotrophs	Sl. No.	Micro-autotrophs
1	<i>Amphiprora</i> sp.##	45	<i>Navicula membranica</i> ##
2	<i>Asterionella japonica</i> ##	46	<i>N. granii</i> ##
3	<i>Asterionellopsis glacialis</i> ##	47	<i>N. delicatula</i> ##
4	<i>Bacteriastrium elongatum</i> ##	48	<i>Navicula</i> sp.##
5	<i>B. furcatum</i> ##	49	<i>Nitzschia longissima</i> ##
6	<i>B. hyalinum</i> ##	50	<i>N. striata</i> ##
7	<i>Bacteriastrium</i> sp.##	51	<i>Nitzschia</i> sp.##
8	<i>Cerataulina pelagica</i> ##	52	<i>Odontella mobiliensis</i> ##
9	<i>Chaetoceros affinis</i> **	53	<i>O. sinensis</i> ##
10	<i>C. brevis</i> **	54	<i>Odontella</i> sp.##
11	<i>C. compressus</i> \$\$	55	<i>Planktoniella sol</i> ##
12	<i>C. curvisetus</i> **	56	<i>Pleurosigma directum</i> ##
13	<i>C. decipiens</i> **	57	<i>P. elongatum</i> ##
14	<i>C. eibenii</i> ##	58	<i>Pleurosigma</i> sp.##
15	<i>C. lorenzianus</i> ##	59	<i>Pseudo-nitzschia seriata</i> ##
16	<i>Chaetoceros</i> sp.##	60	<i>Pseudo-nitzschia</i> sp.##
17	<i>Climacodium</i> sp.##	61	<i>Rhizosolenia alata</i> ##
18	<i>Corethron</i> sp.##	62	<i>R. imbricata</i> **
19	<i>Coscinodiscus asteromphalus</i> **	63	<i>R. robusta</i> **
20	<i>C. excentricus</i> ##	64	<i>R. setigera</i> ##
21	<i>C. granii</i> **	65	<i>R. styliiformis</i> ##
22	<i>C. radiates</i> ##	66	<i>Rhizosolenia</i> sp.##
23	<i>C. wailesii</i> **	67	<i>Skeletonema costatum</i> ##
24	<i>Coscinodiscus</i> sp.##	68	<i>S. marinoi</i> ##
25	<i>Cyclotella</i> sp.##	69	<i>Stephanopyxis</i> sp.##
26	<i>Cylindrotheca</i> sp.##	70	<i>Streptothaca</i> sp.##
27	<i>Dactyliosolen</i> sp.##	71	<i>Surirella</i> sp.##
28	<i>Delphineis</i> sp.##	72	<i>Thalassionema frauenfeldii</i> ##
29	<i>Detonula</i> sp.##	73	<i>T. nitzchioides</i> ##
30	<i>Ditylum brightwellii</i> ##	74	<i>Thalassiosira subtilis</i> ##
31	<i>Eucampia zodiacus</i> ##	75	<i>Thalassiosira</i> sp.##
32	<i>Eucampia</i> sp.##	76	<i>Thalassiothrix</i> sp.##
33	<i>Fragilariopsis</i> sp.##	77	<i>Triceratium</i> sp.##
34	<i>Guinardia flaccid</i> ##	78	<i>Trichodesmium erythraeum</i> \$\$
35	<i>G. striata</i> ##	79	<i>Ceratium furca</i> ##
36	<i>Hemiaulus sinensis</i> ##	80	<i>C. fusus</i> ##
37	<i>Hemiaulus</i> sp.##	81	<i>C. macroceros</i> **
38	<i>Haslea</i> sp.##	82	<i>C. tripos</i> **
39	<i>Hemidiscus hardmanianus</i> **	83	<i>Ceratium</i> sp.##
40	<i>Lauderia annulata</i> ##	84	<i>Dinophysis acuminata</i> ##
41	<i>Leptocylindrus danicus</i> ##	85	<i>D. caudate</i> ##
42	<i>Leptocylindrus</i> sp.##	86	<i>Polysphaeridium</i> sp.\$\$
43	<i>Melosira sulcata</i> ##	87	<i>Prorocentrum</i> sp.##
44	<i>Meuniera</i> sp.##	88	<i>Dictyocha</i> sp.##

Table 3 - Microautotrophs indications in the nearshore waters associated with the coastal upwelling along the southwest coast of India during the Southwest Monsoon. Abbreviations PSWM - Pre-Southwest Monsoon, SWM - Southwest Monsoon

Sl. No.	PSWM (Low nutrient)	SWM (nutrient enriched)
1	Individual cells of <i>Thalassiosira</i>	Colonies of <i>Thalassiosira</i>
2	Shorter chains of <i>Fragilariopsis</i>	Long ribbons of <i>Fragilariopsis</i>
3	Less <i>Thalassionema</i> cells per colony (<4)	More <i>Thalassionema</i> cells per colony (>16)
4	Isolated cells or short chains of <i>Streptotheca</i>	Longer and mats of <i>Streptotheca</i>
5	Less <i>Asterionellopsis</i> cells per colony (<10)	Long spirals numerous cells of <i>Asterionellopsis</i> sp. (>30 cells/colony)
6	Smaller sized species of <i>Chaetoceros</i>	Larger species of <i>Chaetoceros</i> forming longer filaments
7	Shorter filaments of <i>Bacteriastrum</i>	Longer filaments of <i>Bacteriastrum</i>
8	Isolated cells and smaller species of <i>Ceratium</i>	Chains of large-sized <i>Ceratium</i> .
9	Absence of <i>Hemidiscus</i>	The high abundance of <i>Hemidiscus</i>
10	Less abundance of <i>Coscinodiscus</i>	The high abundance of <i>Coscinodiscus</i>
11	Less no. of <i>Rhizosolenia</i>	The high abundance of <i>Rhizosolenia</i>
12	Less no. of <i>Stephanopyxis</i>	Chains of <i>Stephanopyxis</i>
13	Less no. of <i>Guinardia striata</i>	High abundance of <i>Guinardia striata</i>
14	Absence of colonial dinoflagellate <i>Polykrikos</i>	Presence of colonies of <i>Polykrikos</i>

Table 4 - Abundance and size of microautotrophs showing the variations between the Pre- Monsoon and Southwest Monsoon. The values presented as mean \pm standard error. - represents absence. Abbreviations: PSWM - Pre-Southwest Monsoon, SWM - Southwest Monsoon

Micro-phytoplankton	PSWM		SWM	
	Abundance (individual/L)	Mean Size (μm^3 /individual)	Abundance (individual/L)	Mean Size (μm^3 / individual)
<i>Asterionellopsis</i>	2053 \pm 1729	35807 \pm 324	8394 \pm 5026	155540 \pm 14089
<i>Cerataulina</i>	215 \pm 0	46138 \pm 3413	1652 \pm 1392	61031 \pm 911
<i>Ceratium</i>	3304 \pm 2005	38169 \pm 106	1783 \pm 973	431565 \pm 16271
<i>Chaetoceros</i>	1542 \pm 1235	27517 \pm 363	5280 \pm 2940	45715 \pm 1273
<i>Coscinodiscus</i>	9 \pm 3	166 \pm 15.8 ($\times 10^4$)	301 \pm 127	251 \pm 1.3 ($\times 10^4$)
<i>Dinophysis</i>	95 \pm 60	35199 \pm 568	1352 \pm 735	49735 \pm 230
<i>Eucampia</i>	6 \pm 3	21848 \pm 2651	147 \pm 90	25896 \pm 592
<i>Fragilariopsis</i>	69 \pm 39	43367 \pm 1031	908 \pm 334	272997 \pm 5071
<i>Guinardia</i>	67 \pm 14	44435 \pm 2105	2289 \pm 1637	59164 \pm 558
<i>Lauderia</i>	82 \pm 57	45335 \pm 1101	370 \pm 149	65592 \pm 346
<i>Leptocylindrus</i>	619 \pm 454	18183 \pm 343	4741 \pm 3391	33777 \pm 2269
<i>Meuniera</i>	10 \pm 3	46776 \pm 12159	23 \pm 10	80994 \pm 517
<i>Navicula</i>	83 \pm 50	22484 \pm 1054	150 \pm 71	29289 \pm 396
<i>Nitzschia</i>	80 \pm 70	19181 \pm 862	111 \pm 48	39521 \pm 1025
<i>Odontella</i>	1549 \pm 1005	52616 \pm 753	4822 \pm 3340	55952 \pm 615
<i>Pleurosigma</i>	254 \pm 227	25454 \pm 818	245 \pm 152	81840 \pm 1329
<i>Polysphaeridium</i>	30 \pm 4	39967 \pm 2681	-	-
<i>Prorocentrum</i>	99 \pm 47	19320 \pm 194	105 \pm 56	21246 \pm 74
<i>Pseudo-nitzschia</i>	347 \pm 203	18118 \pm 605	2214 \pm 1076	19100 \pm 1193
<i>Rhizosolenia</i>	69 \pm 27	28556 \pm 1454	2442 \pm 1927	79817 \pm 2656
<i>Skeletonema</i>	352 \pm 163	17463 \pm 322	2181 \pm 1136	17773 \pm 562
<i>Streptotheca</i>	132 \pm 55	95140 \pm 2476	161 \pm 94	192350 \pm 348
<i>Stephanopyxis</i>	3 \pm 1	36633 \pm 5128	45 \pm 5	162183 \pm 1529
<i>Thalassionema</i>	243 \pm 164	24928 \pm 712	772 \pm 351	90257 \pm 8025
<i>Thalassiosira</i>	514 \pm 219	64118 \pm 874	2561 \pm 963	102556 \pm 3075
<i>Trichodesmium</i>	1427 \pm 1286	122187 \pm 2256	18 \pm 3	227036 \pm 1622